**Full Paper:** Silsesquioxanes obtained by the hydrolytic condensation of (3-glycidoxypropyl)trimethoxysilane (GPMS) in diglycidyl ether of bisphenol A (DGEBA) were characterized by electrospray ionization time-of-flight mass spectrometry (ESI-TOF MS) and matrix-assisted ultraviolet laser desorption/ionization time-of-flight mass spectrometry (UV-MALDI-TOF MS), employing two different matrices and both positive and negative ion modes. A bimodal distribution of molar masses, in the 1300–6400 *m*/*z* range, was observed in MALDI mass spectra. This distribution accounted for oligomers formed in two successive generations but did not include a cluster of higher molar-mass species present in SEC chromatograms. Most of the peaks present in ESI and MALDI mass spectra could be described by the generic formula $T_n(OCH_3)_m$, with $m$ = 0, 2, and 4 for $n$ = even, $m$ = 1, 3, 5 for $n$ = odd, and T = $RSiO_{(3n-m)/2n}$. This corresponds to completely condensed polyhedra ($m$ = 0), incompletely hydrolyzed polyhedra ($m$ = 1 to 3), and their precursors ($m$ = 4). Predominant species in the first cluster contained 10 to 14 Si atoms whereas those in the second cluster had 18 to 23 Si atoms. Small amounts of the following species: $T_8(OH)(OCH_3)$, $T_9(OH)$, $T_{10}(OH)(OCH_3)$, and $T_{11}(OH)$ could be identified in MALDI MS, using 9H-pyrido[3,4-b]indole (nor-harmane) as matrix in the negative ion mode. It was inferred that some of these species had a relevant participation in the generation of the second cluster of higher molar masses. The stability of the silsesquioxane solution in DGEBA was the result of the very small concentration of free SiOH groups available for further condensation.

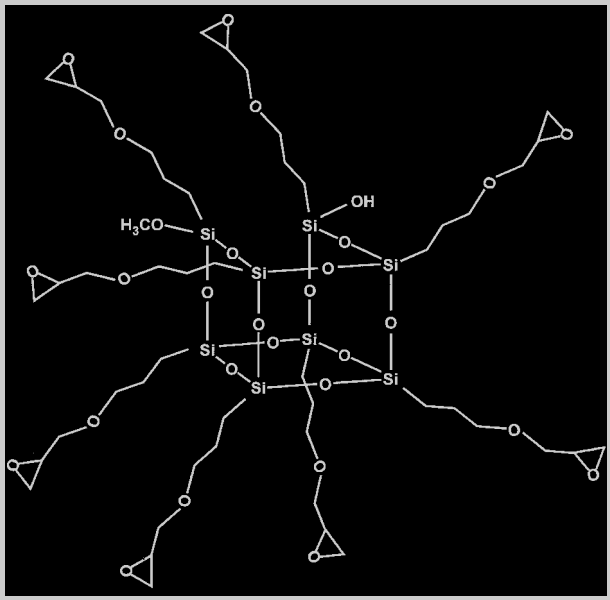


A possible isomer of the key species $T_8(OH)(OCH_3)$.

# UV-MALDI-TOF and ESI-TOF Mass Spectrometry Characterization of Silsesquioxanes Obtained by the Hydrolytic Condensation of (3-Glycidoxypropyl)-trimethoxysilane in an Epoxidized Solvent

*Roberto J. J. Williams,*[1] Rosa Erra-Balsells,*[2] Yoko Ishikawa,[3] Hiroshi Nonami,[3] Adriana N. Mauri,[1] Carmen C. Riccardi*[1]

[1] Institute of Materials Science and Technology (INTEMA), University of Mar del Plata-CONICET, J. B. Justo 4302, 7600 Mar del Plata, Argentina
E-mail: williams@fi.mdp.edu.ar
[2] Department of Organic Chemistry, University of Buenos Aires, Pab. 2, Ciudad Universitaria, 1428 Buenos Aires, Argentina
E-mail: erra@qo.fcen.uba.ar
[3] Plant Biophysics/Biochemistry Research Laboratory, College of Agriculture, Ehime University, Matsuyama 790-8566, Japan

## Introduction

The hydrolytic condensation of trialkoxysilanes, $RSi(OR')_3$, performed in the presence of water and an acid or a base as catalysts, leads to products that are generically called poly(silsesquioxanes) or silsesquioxanes.[1] Their structure may vary from perfect polyhedra of formula $(RSiO_{1.5})_n$ ($n$ = even number $\geqslant 6$), also denoted as $T_n$ or POSS (polyhedral oligomeric silsesquioxanes), to partially hydrolyzed/condensed products of generic formula $T_n(OH)_x(OR')_y$ where T = $RSiO_{1.5-(x+y)/2n}$. Figure 1 shows different structures of silsesquioxanes.

  1022-1352/2001/1107–2425$17.50+.50/0

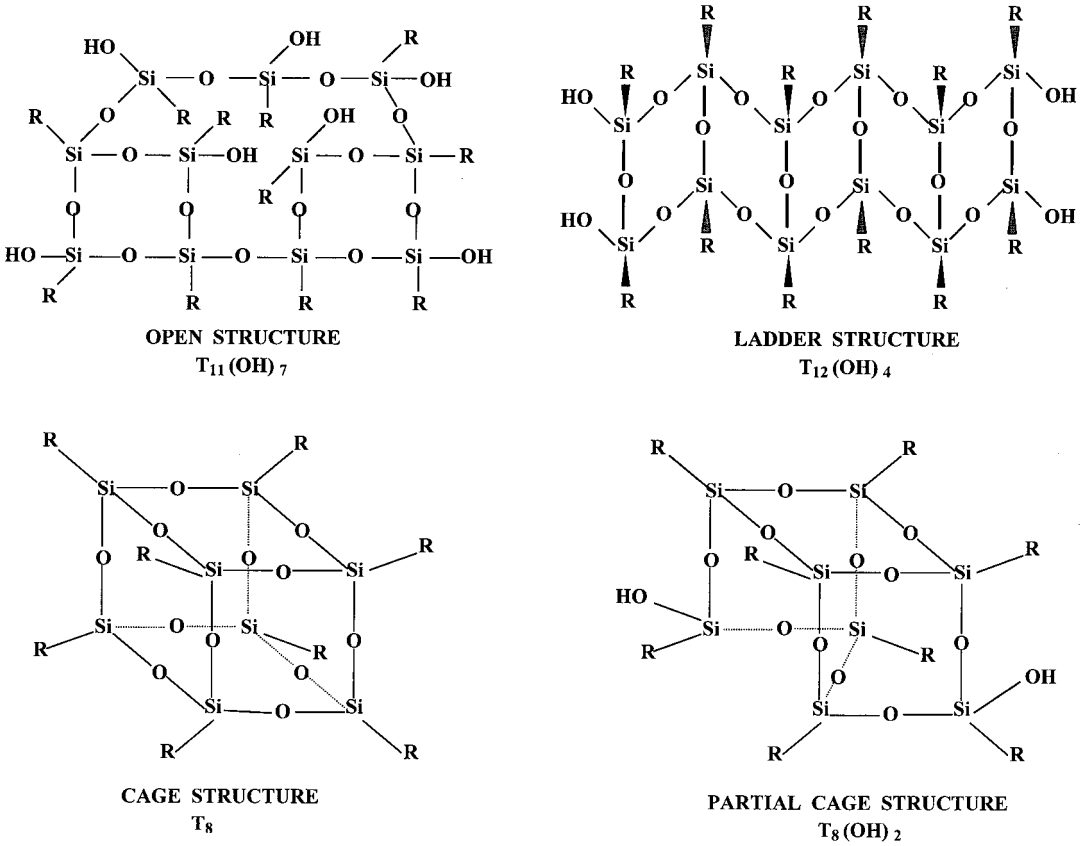


Figure 1. Generic structures of silsesquioxanes.

The first generation of products formed in the reaction may be identified and, eventually, isolated.[2–5] But the structure of higher oligomers and the reaction path leading to them are basically unknown. A progress in this regard has been made through the use of advanced mass spectrometry (MS) techniques. Hong et al.[6] reported the characterization of highly charged dendrimers with encapsulated cuboid octasilsesquioxanes and molar masses up to about 5500, using electrospray ionization (ESI MS). Bakhtiar at al.[7,8] reported the mass spectrometric characterization of polyhedral oligosilsesquioxanes and their metal-containing derivatives (with Si—O—M bonds), using atmospheric pressure chemical ionization (APCI) and turbo ion-spray (TISP) mass spectrometry. Wallace et al.[9,10] used matrix-assisted ultraviolet laser desorption/ionization time-of-flight mass spectrometry (UV-MALDI-TOF MS) to characterize broad molar mass distributions of incompletely condensed silsesquioxanes derived from various trialkoxysilanes. The degree of intramolecular condensation was established for the different series of oligomers. Eisenberg et al.[11] used UV-MALDI-TOF MS to determine the molar mass distribution of silsesquioxanes derived from the hydrolytic condensation of (3-methacryloxypropyl)trimethoxysilane (MPMS). The distribution was multimodal with different peaks corresponding to oligomers formed in successive generations. During the initial stage of the polycondensation, oligomers with 7–12 Si atoms were produced. They mainly consisted of incompletely condensed polyhedra (species with 1–3 OH per molecule). Species with more OH groups were condensed with a higher probability, giving place to a second generation of oligomers. Third and fourth generations of condensation products were also evidenced.

Silsesquioxanes derived from (3-glycidoxypropyl)trimethoxysilane, synthesized under different experimental conditions, were characterized by size exclusion chromatography (SEC).[11–14] Multimodal distributions were found, with a first cluster of species assigned to cage-like structures including the (incompletely condensed) octahedron as a fundamental building block for the generation of successive clusters. A recent paper by Matejka et al.[13] reported the use of ESI MS to characterize species present in the first cluster. They confirmed the presence of polyhedra and incompletely hydrolyzed/condensed polyhedra (cage-like structures), containing 8–11 Si atoms. The octahedron was the species present in a higher concentration. However, no precise assignment of the whole distribution could be made due to the partial hydrolysis or methanolysis of epoxy groups occurring during the synthesis. This is the result of the difficulty in keeping the integrity of epoxy groups in the presence of the usual catalysts employed to produce the hydrolytic condensation of (3-glycidoxypropyl)trimethoxysilane.[12, 13, 15]

In previous studies [11, 14] we reported the synthesis of a silsesquioxane derived from (3-glycidoxypropyl)trimethoxysilane (GPMS), using diglycidyl ether of bisphenol A (DGEBA) as a solvent. A multimodal distribution of molar masses was evidenced by size exclusion chromatography (SEC), with relative maxima for species with 4, 8, 24 Si atoms (based on a calibration with PS standards), together with a broad peak at high molar masses (maximum at about 24 000). In spite of the large molar masses attained in the synthesis, the solution was significantly stable (no gelation was observed during the heating up to 140 °C or after prolonged periods of storage at room temperature). An interesting characteristic of this silsesquioxane was the fact that the epoxy rings of both GPMS and DGEBA remained intact during the synthesis, as revealed by $^1$H-NMR within the experimental accuracy of this technique. This was proved by the constancy of the ratio of the number of protons of the epoxy ring in DGEBA (2.68, 2.79, and 3.85 ppm) and in GPMS (2.52, 2.69, and 3.32 ppm), with respect to the number of protons of aromatic rings in DGEBA (6.87 and 7.21 ppm) and the $\alpha$-$CH_2$ group in GPMS (0.64 ppm).[11] A rather unusual fact was the presence of a significant amount of residual ($OCH_3$) groups in the structure of the final silsesquioxane. By $^1$H-NMR it was estimated that about 7% of the initial Si—$OCH_3$ groups were not hydrolyzed under the selected reaction conditions.[11] The silsesquioxane-modified DGEBA may be used as a starting monomer to synthesize different types of epoxy networks.

The aim of this study is to use a combination of ESI-TOF MS and UV-MALDI-TOF MS (with two different matrices and using positive and negative ion modes), to obtain an accurate description of the main species present in the silsesquioxane dissolved in DGEBA. We will try to explain the reasons for the high stability of the solution and to infer some of the key steps in the reaction path.

## Experimental Part

*Synthesis of Silsesquioxanes*

A detailed description of the synthesis was reported elsewhere.[11, 14] Basically, the hydrolytic condensation of (3-glycidoxypropyl)trimethoxysilane (GPMS, Sigma) was performed in solution using diluted formic acid as a catalyst (molar ratio $H_2O$/Si = 3). A first step was carried out in tetrahydrofuran (THF), and the final step where most of the large-molar-mass species were generated, was made using diglycidyl ether of bisphenol A (DGEBA, MY790 Ciba) as a solvent (50% of the total number of epoxy groups were supplied by the solvent). Temperature was increased in steps, with a final step carried out at $T$ = 140 °C (most of the catalyst, water, and THF were eliminated in this process).

*Characterization Employing ESI-TOF MS*

The positive-ion electrospray ionization time-of-flight (ESI-TOF) mass spectra were acquired by directly infusing the polymers solution (0.1 mg/mL methanol-THF 1 : 1; solvents: Aldrich, HPLC grade) into the ESI ion source of the Mariner PerSeptive Biosystems ESI-TOF mass spectrometer. The $m/z$ range of the mass spectrometer was 500–2 500 Da. Methanol-THF 1 : 1 was used as solvent stream. The spray tip potential was +2 695.9 V, the nozzle potential was +120.1 V, and the skimmer voltage was +12.01 V. Nozzle temperature was 140 °C. A Harvard PHD 2000 syringe infusion pump at a flow-rate of 10 μL · min$^{-1}$ was used for polymer solution introduction. The nitrogen flow rate was 0.35–0.41 L · min$^{-1}$. The analyzer temperature was kept at 31.7 °C and pressure at 0.55 MPa. The mass calibration was achieved by using $\beta$-cyclodextrin (Sigma) (0.0227 mg/mL methanol-water 9 : 1; water: Milli-Q grade). All the significant peaks present in the mass spectra, e. g. with relative intensities in the 10–100% range, corresponded to species ionized with sodium ($M+Na^+$) ($z$ = 1) and ($M+2Na^+$) ($z$ = 2).

*Characterization by UV-MALDI-TOF MS*

Matrix-assisted ultraviolet laser desorption/ionization time-of-flight mass spectrometry was performed using a Shimadzu Kratos, Kompact MALDI 4 device with pulsed extraction and tunable time delay capability. It was equipped with a pulsed nitrogen laser ($\lambda$ = 337 nm; pulse width = 3 ns). TOF analyzers were used at 20 kV, and ions were obtained by irradiation just above the threshold laser power. Samples were measured in the linear mode, in both positive and negative ion modes. Usually 50 spectra were accumulated.

Several chemicals were used as matrices: 2-(4-hydroxyphenylazo)benzoic acid (HABA); *trans*-3-indoleacrylic acid (IAA); 2,5-dihydroxybenzoic acid (gentisic acid, GA) and 9H-pyrido[3,4-b]indole (nor-harmane, nor-Ho)[16, 17] (Sigma), to elucidate the possible interference of solvent (DGEBA) and matrix aggregates on the mass spectra. Only results obtained with both nor-Ho and HABA will be reported because they exhibited no interference by the solvent or matrix. All peaks obtained in the positive mode could be assigned to ($M+Na^+$) species, and those obtained in the negative mode to ($M-H^+$) species.

Both the matrix and the silsesquioxane solution in DGEBA were dissolved in THF (Aldrich, HPLC grade), and mixed together in different volumetric ratios. Two coatings (0.5 μL each) were performed on the sample probe tip, and solvent was removed by blowing air at room temperature after each one of the coatings. In every experiment, mixtures of the matrix and DGEBA in THF were also monitored.

Several proteins (Sigma) dissolved in aqueous 0.1% TFA (Merck) and cyclodextrins (Sigma) in water (Milli-Q grade) solution were used for calibration purposes.

## Results and Discussion

*ESI-TOF Mass Spectra*

Figure 2 shows the ESI-TOF mass spectrum in the 750–2 500 $m/z$ range, and Table 1 shows the assignment of peaks, in decreasing order of intensities up to about 20% of the maximum value. Theoretical masses were calcu-

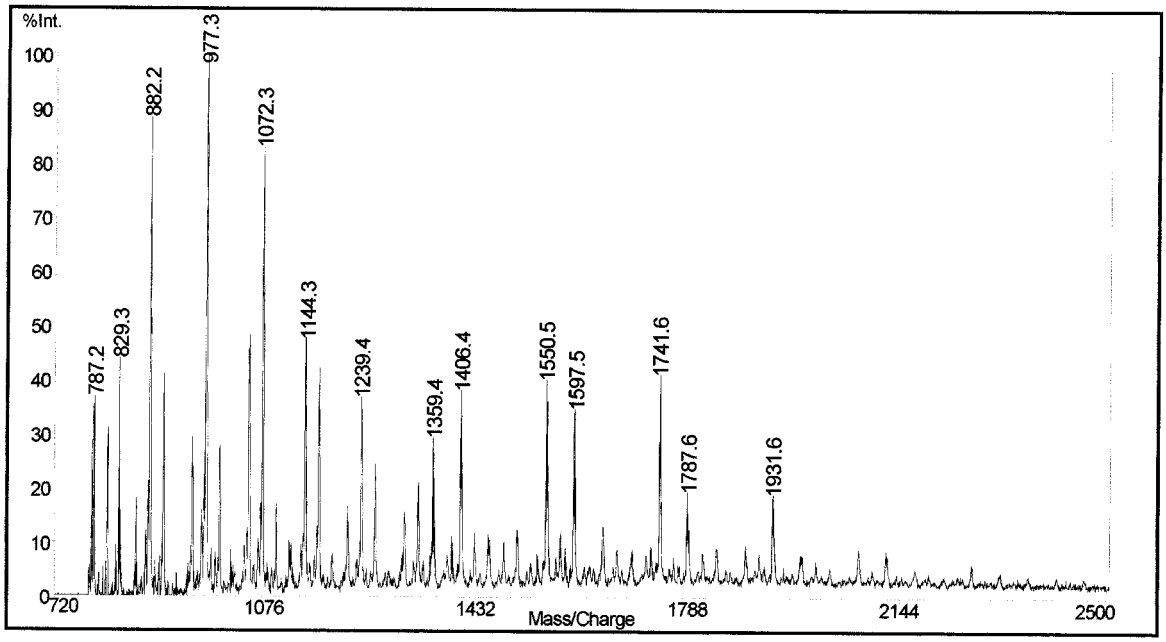


Figure 2. ESI-TOF mass spectrum (positive ion mode) in the 750–2 500 *m/z* range.

Table 1. Assignment of ESI-TOF MS peaks in decreasing order of intensity (positive ion mode).

| Exptl. *m/z* | *z* | Intensity | Assignment | Predicted $(M+zNa^+)/z$ |
|---|---|---|---|---|
| 977.3 | 2 | 100 | $T_{11}(OCH_3)_3$ | 977.3 |
| 882.2 | 2 | 88 | $T_{10}(OCH_3)_2$ | 882.2 |
| 1 072.3 | 2 | 83 | $T_{12}(OCH_3)_4$ | 1 072.5 |
| 1 049.3 | 2 | 48 | $T_{12}(OCH_3)_2$ | 1 049.4 |
| 1 144.3 | 2 | 48 | $T_{13}(OCH_3)_3$ | 1 144.6 |
| 829.3 | 1 | 44 | $T_4(OCH_3)_6$ | 830.1 |
| 1 167.3 | 2 | 42 | $T_{13}(OCH_3)_5$ | 1 167.6 |
| 904.8 | 2 | 41 | $T_{10}(OCH_3)_4$ | 905.2 |
| 1 740.6; 1 741.6 | 1 | 41 | $T_{10}(OCH_3)_2$ | 1 741.4 |
| 1 550.5; 1 551.5 | 1 | 40 | $T_9(OCH_3)$ | 1 551.1 |
| 1 406.4 | 1 | 38 | $T_8(OCH_3)_2$ | 1 406.9 |
| 1 239.4 | 2 | 37 | $T_{14}(OCH_3)_4$ | 1 239.7 |
| 786.2; 787.2 | 2 | 37 | $T_9(OCH_3)$ | 787.1 |
| 1 597.5 | 1 | 35 | $T_9(OCH_3)_3$ | 1 597.2 |
| 810.2 | 2 | 31 | $T_9(OCH_3)_3$ | 810.1 |
| 954.3 | 2 | 30 | $T_{11}(OCH_3)$ | 954.3 |
| 1 359.4 | 1 | 30 | $T_8$ | 1 360.9 |
| 783.3 | 1 | 29 | $T_4(OCH_3)_4$ | 784.1 |
| 999.8; 1 000.3 | 2 | 27 | $T_{11}(OCH_3)_5$ | 1 000.4 |
| 1 262.4 | 2 | 24 | $T_{14}(OCH_3)_6$ | 1 262.7 |
| 1 334.9 | 2 | 21 | $T_{15}(OCH_3)_5$ | 1 334.9 |
| 1 787.6 | 1 | 20 | $T_{10}(OCH_3)_4$ | 1 787.5 |
| 1 930.6; 1 931.6 | 1 | 19 | $T_{11}(OCH_3)_3$ | 1 931.7 |

lated using the average isotopic composition of the proposed compounds. The reproducibility of the mass spectrum was excellent, except for a few peaks that were shifted in 1 *m/z* unit in different runs, as indicated in Table 1. The shift was ascribed to a very close concentration of different isotopes in the range of the average value. The agreement between theoretical and experimental values is excellent and comprised within the experimental error of the technique.

All the species present in significant concentrations in the explored *m/z* range have the generic formula $T_n(OCH_3)_m$ where $T = RSiO_{1.5-m/2n}$. The generation of these species can be ascribed to the following reactions:

$$T_x(OCH_3)_y + H_2O \rightarrow T_x(OCH_3)_{y-1}(OH) + CH_3OH \quad (1)$$

$$T_x(OCH_3)_{y-1}(OH) + T_{n-x}(OCH_3)_{m+2-y} \rightarrow T_n(OCH_3)_m + CH_3OH \quad (2)$$

The absence of significant concentrations of species with SiOH groups means that the condensation step Equation (2) proceeded with a much higher rate than the hydrolysis step Equation (1). This also explains the high stability of the silsesquioxane during its heating to 140 °C (residual water and formic acid are evaporated during this stage).

The silsesquioxane solution in DGEBA may be used to form an inorganic network (Si—O—Si bonds) through the addition of water and a catalyst, or an organic network based on the polymerization of the epoxy groups through different possible mechanisms, or both of them, simultaneously or sequentially. Properties of materials based on the organic network, e.g. silsesquioxane-modified epoxies, are reported elsewhere.[14, 18] Both the elastic modulus in the rubbery state and the abrasion resistance are significantly enhanced.

Most of the species present in the ESI-TOF mass spectrum belong to the cluster of oligomers associated to the first significant peak in the SEC chromatogram of the silsesquioxane.[11, 14] We will refer to this cluster as the first generation of species to differentiate it from clusters of higher molar-mass species, formed in successive genera-

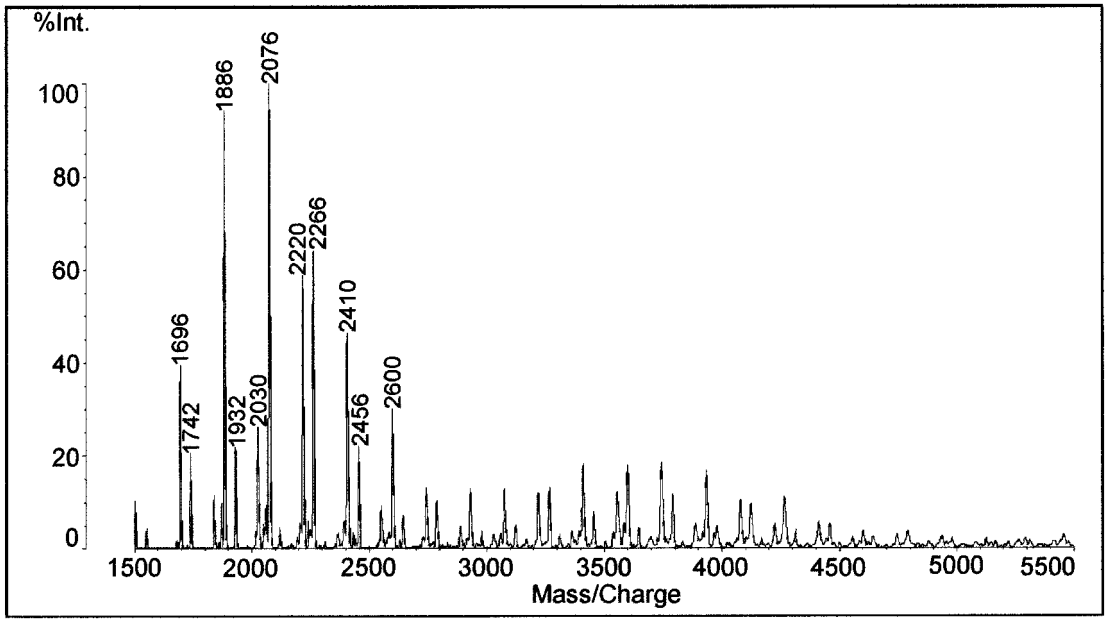


Figure 3. UV-MALDI-TOF mass spectrum (positive ion mode) in the 1 500–5 500 range, using nor-Ho as matrix.

Table 2. Assignment of UV-MALDI-TOF MS peaks belonging to the first cluster, in decreasing order of intensity (matrix = nor-Ho; positive ion mode).

| Exptl. *m/z* | Intensity | Assignment | Predicted ($M+Na^+$) |
|---|---|---|---|
| 2076 | 100 | $T_{12}(OCH_3)_2$ | 2076 |
| 1886 | 94 | $T_{11}(OCH_3)$ | 1886 |
| 2266 | 64 | $T_{13}(OCH_3)_3$ | 2266 |
| 2220 | 59 | $T_{13}(OCH_3)$ | 2220 |
| 2410 | 47 | $T_{14}(OCH_3)_2$ | 2410 |
| 1696 | 39 | $T_{10}$ | 1695 |
| 2600 | 30 | $T_{15}(OCH_3)_3$ | 2601 |
| 2030 | 26 | $T_{12}$ | 2030 |
| 2456 | 22 | $T_{14}(OCH_3)_4$ | 2456 |
| 1932 | 21 | $T_{11}(OCH_3)_3$ | 1932 |
| 1742 | 20 | $T_{10}(OCH_3)_2$ | 1741 |

tions. A residual amount of a tetramer, also present in the SEC chromatogram, was identified in the mass spectrum. It was assigned to species $T_4(OCH_3)_6$ and $T_4(OCH_3)_4$, which are, respectively, the linear and the cyclic tetramer.

The first generation of species comprised oligomers containing from about 8 to 14 Si atoms. They include polyhedra ($T_8$), incompletely hydrolyzed polyhedra (species containing 1 to 3 methoxy groups), and their precursors (species with 4 or more methoxy groups). The following species were present in significantly high concentrations: $T_{10}(OCH_3)_2$, $T_{11}(OCH_3)_3$, and $T_{12}(OCH_3)_4$.

### *UV-MALDI-TOF Mass Spectra*

This technique enables to extend the analysis to a broader range of molar masses. Figure 3 shows the UV-MALDI-TOF mass spectrum in the 1 500–5 500 *m/z* range, using nor-Ho as matrix. The presence of two clusters of species corresponding to the first and second generation of oligomers is clearly evidenced, in spite of the mass discrimination in MALDI MS (in SEC chromatograms, the second cluster of species was larger than the first one, and the third cluster of high molar masses is not even detected by MALDI MS).[11, 14]

Table 3. Assignment of UV-MALDI-TOF MS peaks belonging to the second cluster, in decreasing order of intensity (matrix = nor-Ho; positive ion mode).

| Exptl. *m/z* | Intensity | Assignment | Predicted ($M+Na^+$) |
|---|---|---|---|
| 3746 | 100 | $T_{22}(OCH_3)_2$ | 3748 |
| 3601 | 97 | $T_{21}(OCH_3)_3$ | 3604 |
| 3411 | 96 | $T_{20}(OCH_3)_2$ | 3414 |
| 3935 | 91 | $T_{23}(OCH_3)_3$ | 3938 |
| 2745 | 69 | $T_{16}(OCH_3)_2$ | 2745 |
| 3268 | 69 | $T_{19}(OCH_3)_3$ | 3269 |
| 2934 | 68 | $T_{17}(OCH_3)_3$ | 2935 |
| 3079 | 68 | $T_{18}(OCH_3)_2$ | 3079 |
| 3556 | 67 | $T_{21}(OCH_3)$ | 3558 |
| 3222 | 63 | $T_{19}(OCH_3)$ | 3223 |
| 3791 | 62 | $T_{22}(OCH_3)_4$ | 3794 |
| 4268 | 58 | $T_{25}(OCH_3)_3$ | 4273 |
| 4080 | 57 | $T_{24}(OCH_3)_2$ | 4083 |
| 2791 | 54 | $T_{16}(OCH_3)_4$ | 2791 |
| 4125 | 52 | $T_{24}(OCH_3)_4$ | 4129 |
| 3457 | 42 | $T_{20}(OCH_3)_4$ | 3460 |
| 4413 | 31 | $T_{26}(OCH_3)_2$ | 4417 |
| 3890 | 29 | $T_{23}(OCH_3)$ | 3892 |
| 4225 | 29 | $T_{25}(OCH_3)$ | 4227 |
| 4460 | 28 | $T_{26}(OCH_3)_4$ | 4463 |
| 3124 | 27 | $T_{18}(OCH_3)_4$ | 3125 |

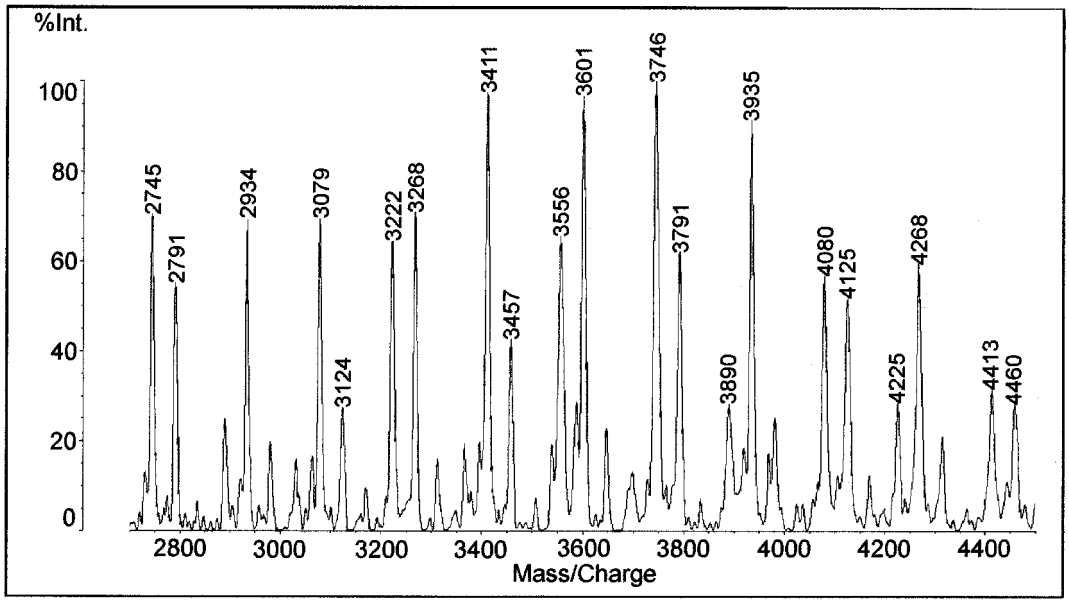


Figure 4. Amplification of the UV-MALDI-TOF mass spectrum (positive ion mode) in the 2 700–4 500 *m/z* range, using nor-Ho as matrix.

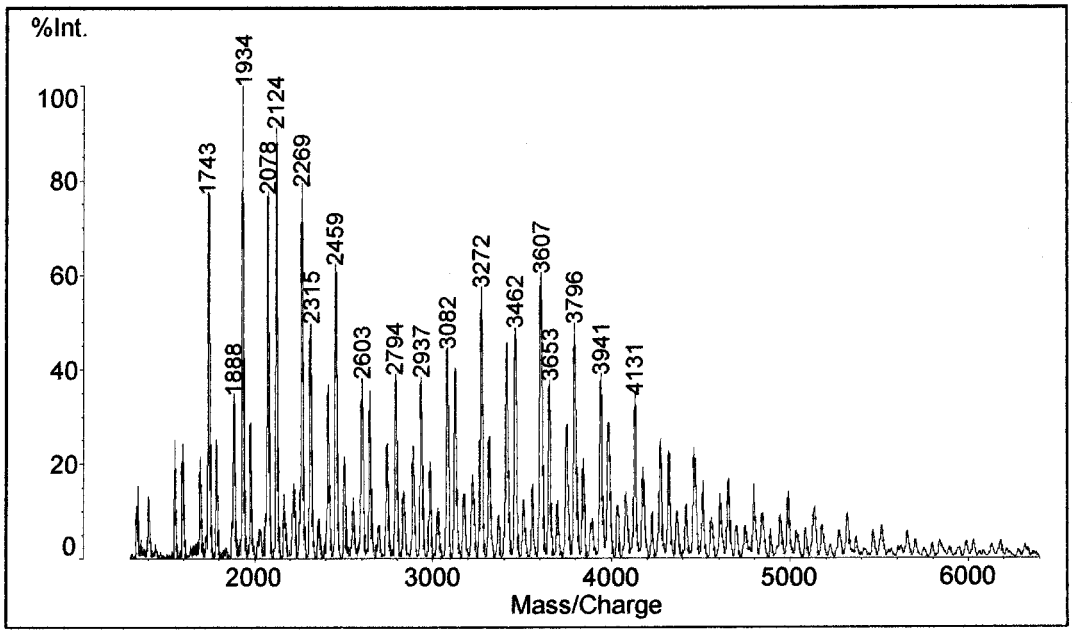


Figure 5. UV-MALDI-TOF mass spectrum (positive ion mode) in the 1 300–6 500 *m/z* range, using HABA as matrix.

Table 2 shows the assignment of peaks of the first cluster, in decreasing order of intensities up to about 20% of the maximum value. Theoretical masses were calculated using the average isotopic composition of the proposed compounds. Again, an excellent agreement was found between experimental and predicted values.

Peaks present in significant concentrations in the first cluster may be described by the generic formula $T_n(OCH_3)_m$, in agreement with ESI-TOF MS results. However, more condensed species appear in high concentrations in MALDI mass spectra using nor-Ho as matrix. Polyhedra ($T_{10}$ and $T_{12}$) and incompletely hydrolyzed polyhedra like $T_{13}(OCH_3)$, $T_{14}(OCH_3)_2$, and $T_{15}(OCH_3)_3$, are present in relatively high concentrations in the MALDI mass spectrum and were not recorded among the significant species present in the ESI mass spectrum.

Figure 4 shows an amplification of the second cluster of species present in the 2 700–4 500 *m/z* range, and Table 3 shows the peaks present in significant concentrations together with their assignment. In this *m/z* range there is a systematic shift, with an average value of about 2 Da, between predicted and experimental values. These small

Table 4. Assignment of UV-MALDI-TOF MS in decreasing order of intensity (matrix = HABA; positive ion mode).

| Exptl. *m/z* | Intensity | Assignment | Predicted ($M+Na^+$) |
|---|---|---|---|
| 1934 | 100 | $T_{11}(OCH_3)_3$ | 1932 |
| 2124 | 91 | $T_{12}(OCH_3)_4$ | 2122 |
| 2269 | 80 | $T_{13}(OCH_3)_3$ | 2266 |
| 1743 | 78 | $T_{10}(OCH_3)_2$ | 1741 |
| 2078 | 78 | $T_{12}(OCH_3)_2$ | 2076 |
| 2459 | 63 | $T_{14}(OCH_3)_4$ | 2456 |
| 3607 | 60 | $T_{21}(OCH_3)_3$ | 3604 |
| 3272 | 57 | $T_{19}(OCH_3)_3$ | 3269 |
| 3796 | 50 | $T_{22}(OCH_3)_4$ | 3794 |
| 2315 | 49 | $T_{13}(OCH_3)_5$ | 2312 |
| 3462 | 48 | $T_{20}(OCH_3)_4$ | 3460 |
| 3416 | 45 | $T_{20}(OCH_3)_2$ | 3414 |
| 3082 | 44 | $T_{18}(OCH_3)_2$ | 3079 |
| 3128 | 40 | $T_{18}(OCH_3)_4$ | 3125 |
| 2794 | 40 | $T_{16}(OCH_3)_4$ | 2791 |
| 3941 | 40 | $T_{23}(OCH_3)_3$ | 3938 |
| 2603 | 39 | $T_{15}(OCH_3)_3$ | 2601 |
| 2413 | 38 | $T_{14}(OCH_3)_2$ | 2410 |
| 2937 | 38 | $T_{17}(OCH_3)_3$ | 2935 |
| 3653 | 37 | $T_{21}(OCH_3)_5$ | 3650 |
| 1888 | 35 | $T_{11}(OCH_3)$ | 1886 |
| 2650 | 35 | $T_{15}(OCH_3)_5$ | 2647 |
| 4131 | 34 | $T_{24}(OCH_3)_4$ | 4129 |
| 1980 | 30 | $T_{11}(OCH_3)_5$ | 1978 |

shifts, in one sense or the other (an example is provided by the MALDI mass spectrum obtained with HABA as matrix), were ascribed to an imprecise calibration.

All the peaks present in significant concentrations in the second cluster correspond to species of generic formula $T_n(OCH_3)_m$. Those with 1 to 3 ($OCH_3$) groups may be represented by cage-like structures whereas those with 4 or more ($OCH_3$) groups may be described as precursors of these structures.

Figure 5 shows the UV-MALDI-TOF mass spectrum in the 1300–6400 *m/z* range, using HABA as matrix. With this matrix there is a much better definition of the second cluster. The assignment of significant peaks is shown in Table 4. The systematic shift of 2–3 Da between experimental and predicted values is in the range of the calibration error.

Again, all species present in significant concentrations contain a few unhydrolyzed ($OCH_3$) groups but no residual SiOH group. An interesting observation is the fact that the five species present in a higher concentration in the first cluster are the same as those recorded with ESI-TOF MS. Only two of these species are recorded among the five more important of the first cluster when using nor-Ho as matrix in MALDI MS. This means that there is a discrimination of the nature of the particular species in the ionization/desorption process that depends on the selected matrix, e. g. nor-Ho seems to be more efficient to detect more condensed species than HABA.

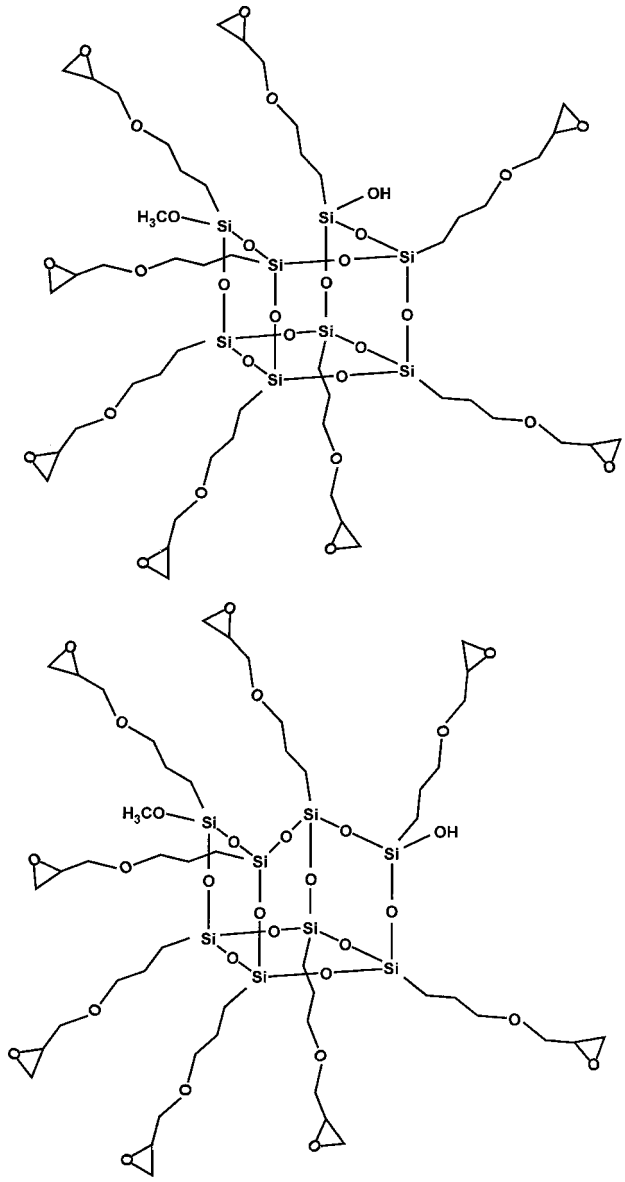


Figure 6. Possible isomers of the key species $T_8(OH)(OCH_3)$.

When following the synthesis of this silsesquioxane using size exclusion chromatography,[11, 14] it was observed that: a) the first cluster was initially rich in species containing 8 Si atoms (based on PS standards), b) the second cluster was generated at the expense of part of the population of the first one. By analyzing the distribution of species shown in Table 4, it was observed that the six species present in a higher concentration in the second cluster can be generated by reaction of the corresponding six species present in a higher concentration in the first cluster, with $T_8(OH)(OCH_3)$. Corresponding reactions are:

$$T_{10}(OCH_3)_2 + T_8(OH)(OCH_3) \rightarrow T_{18}(OCH_3)_2 + CH_3OH \quad (3)$$

$$T_{11}(OCH_3)_3 + T_8(OH)(OCH_3) \rightarrow T_{19}(OCH_3)_3 + CH_3OH \quad (4)$$

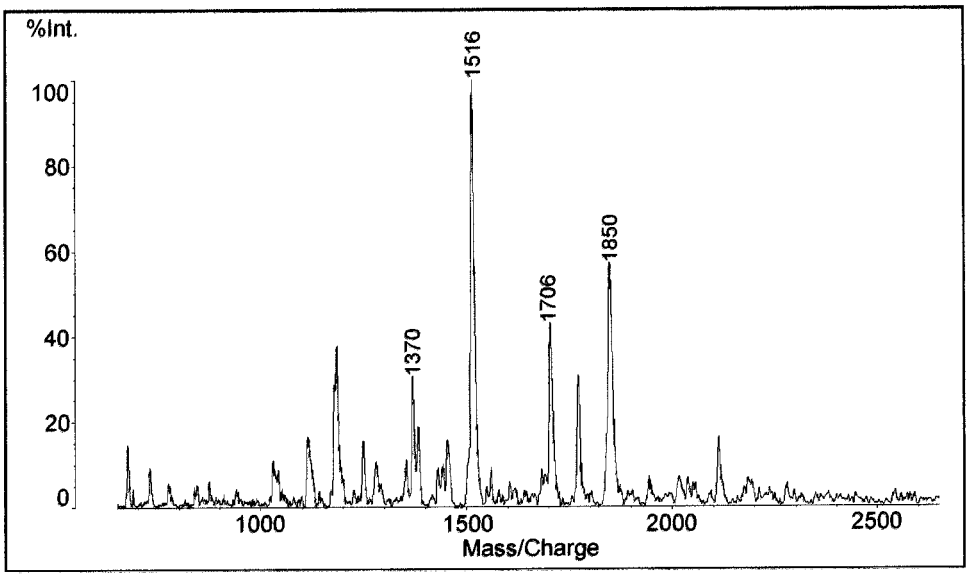


Figure 7. UV-MALDI-TOF mass spectrum (negative ion mode) in the 650–2650 *m/z* range, using nor-Ho as matrix.

$$T_{12}(OCH_3)_2 + T_8(OH)(OCH_3) \rightarrow T_{20}(OCH_3)_2 + CH_3OH \quad (5)$$

$$T_{12}(OCH_3)_4 + T_8(OH)(OCH_3) \rightarrow T_{20}(OCH_3)_4 + CH_3OH \quad (6)$$

$$T_{13}(OCH_3)_3 + T_8(OH)(OCH_3) \rightarrow T_{21}(OCH_3)_3 + CH_3OH \quad (7)$$

$$T_{14}(OCH_3)_4 + T_8(OH)(OCH_3) \rightarrow T_{22}(OCH_3)_4 + CH_3OH \quad (8)$$

Possible isomers of the key species $T_8(OH)(OCH_3)$ are shown in Figure 6. Obviously, other species containing OH groups must be present to account for the broad distribution of species present in the second cluster. The hydrolysis of $Si(OCH_3)$ groups of species belonging to the second cluster and its further condensation with species of the first or second clusters explains the generation of the high-molar-mass peak present in size exclusion chromatograms. At the end of this process no significant concentration of species bearing SiOH groups is observed.

Matejka et al.[12] analyzed the molar mass distribution of a silsesquioxane synthesized from (3-glycidoxypropyl)trimethoxysilane, in bulk at 80 °C, using benzyldimethylamine (BDMA) as catalyst, and a molar ratio $H_2O$/Si = 1.5. After 1 h reaction, a bimodal distribution of molar masses was observed by SEC. ESI-TOF mass spectra showed the presence of the following species belonging to the first cluster (in decreasing order of intensity): $T_8$, $T_8(OH)(OCH_3)$, $T_9(OH)$, $T_9(OH)_2(OCH_3)$, $T_{10}(OCH_3)(OH)$, $T_{10}$, etc. In this case some ambiguity results from the possibility of producing partial hydrolysis or methanolysis of epoxy groups, as stated by the authors. Besides, the homopolymerization of epoxy groups initiated by BDMA may also take place in parallel. In spite of this, it is indeed possible that the identified species containing SiOH groups behave as active intermediates in the generation of the second cluster.

In order to search traces of species with SiOH groups in the silsesquioxane/DGEBA solution, UV-MALDI-TOF mass spectra in the negative mode were recorded using different matrices. Mass spectra of DGEBA and the corresponding matrix were also recorded to discard peaks contributed by the solvent/matrix combination. For most matrices, including HABA, only signals of the solvent/matrix appeared in the spectra, a fact that indirectly indicates the difficulty of extracting a $H^+$ from a $T_n(OCH_3)_m$ species. But when using nor-Ho as matrix, the mass spectrum shown in Figure 7 was obtained. Apart from the peaks contributed by the DGEBA/nor-Ho combination, four extra peaks at *m/z* = 1370, 1516, 1706, and 1850 were detected. They were assigned to the following $(M-H)^-$ species: $T_8(OH)(OCH_3)$, $T_9(OH)$, $T_{10}(OH)(OCH_3)$, and $T_{11}(OH)$, with theoretical values of *m/z* equal to 1369, 1513, 1704, and 1848, respectively. The small shift between measured and predicted values lies in the range of the experimental error. It may be inferred that these species were active intermediates during the synthesis of the silsesquioxane.

Nonami et al.[16, 17] and Erra-Balsells et al.[19] showed that nor-Ho as UV-MALDI matrix allows to see oligosaccharides and proteins as protonated species, $(M+H)^+$, in the positive ion mode, and deprotonated species, $(M-H)^-$, in the negative ion mode. They suggested that the simultaneous presence of the acid indole NH group and the basic pyridine N group in nor-Ho structure accounts for its special behavior.

## Conclusions

The combined use of ESI-TOF MS and UV-MALDI-TOF MS, using two different matrices and positive and

negative operation modes, enabled us to characterize a silsesquioxane based on (3-glycidoxypropyl)trimethoxysilane, synthesized in an epoxidized solvent (DGEBA). Some characteristics of the advanced mass spectrometry techniques as applied to silsesquioxanes could be also discerned.

Most of the species present in significant concentrations in the silsesquioxane had the generic formula $T_n(OCH_3)_m$, distributed in clusters differing in their average molar masses. The absence of SiOH groups was ascribed to the high ratio of condensation vs. hydrolysis rates. Predominant species present in the first cluster were completely condensed polyhedra: $T_8$, $T_{10,}$ and $T_{12}$, incompletely hydrolyzed polyhedra: $T_{10}(OCH_3)_2$, $T_{11}(OCH_3)$, $T_{11}(OCH_3)_3$, $T_{12}(OCH_3)_2$, $T_{13}(OCH_3)$, $T_{13}(OCH_3)_3$, $T_{14}(OCH_3)_2$, and their precursors: $T_{10}(OCH_3)_4$, $T_{12}(OCH_3)_4$, and $T_{14}(OCH_3)_4$. Predominant species present in the second cluster were incompletely hydrolyzed polyhedra: $T_{18}(OCH_3)_2$, $T_{19}(OCH_3)_3$, $T_{20}(OCH_3)_2$, $T_{21}(OCH_3)_3$, $T_{22}(OCH_3)_2$, $T_{23}(OCH_3)_3$, and their precursors: $T_{20}(OCH_3)_4$, $T_{22}(OCH_3)_4$, etc. It was inferred that predominant species of the second cluster were generated by the reaction of predominant species found in the first cluster with active intermediates like $T_8(OH)(OCH_3)$ and $T_{10}(OH)(OCH_3)$. These intermediates could be detected by operating the UV-MALDI-TOF MS in the negative mode and using nor-Ho as matrix. The findings reported in this study explain: a) the high stability of the silsesquioxane/DGEBA solution, derived from the very low concentration of SiOH groups, b) the growth of the second cluster of species at the expense of the first cluster, as observed by SEC. They also confirm the fact that cage-like structures are prevalent in the reaction mixture.[11, 12]

When using nor-Ho as matrix and operating in the negative mode, UV-MALDI-TOF MS could detect species containing SiOH groups in the presence of a large amount of generic species $T_n(OCH_3)_m$, that were not detected by this technique. It was also found that the nature of the selected matrix discriminated among species with different condensation degrees; e.g. nor-Ho exhibited a higher efficiency than HABA to the desorption/ionization of more condensed structures.

*Acknowledgement:* We acknowledge the financial support of *CONICET*, *ANPCyT,* and *Universities of Buenos Aires and Mar del Plata*, Argentina. R. Erra-Balsells, C. C. Riccardi, and R. J. J. Williams are Research Members of *CONICET*. ESI-TOF MS and UV-MALDI-TOF MS experiments were performed as part of the academic agreement between Rosa Erra-Balsells and Hiroshi Nonami with the facilities of the High Resolution Liquid Chromatography-integrated Mass Spectrometer System of the *United Graduated School of Agricultural Sciences* (Ehime University, Japan).

Received: November 7, 2000
Revised: January 4, 2001

[1] R. H. Baney, M. Itoh, A. Sakakibara, T. Suzuki, *Chem. Rev.* **1995**, *95*, 1409.
[2] J. F. Brown, Jr., L. H. Vogt, Jr., P. I. Prescott, *J. Am. Chem. Soc.* **1964**, *86*, 1120.
[3] J. F. Brown, Jr., L. H. Vogt, Jr., *J. Am. Chem. Soc.* **1965**, *87*, 4313.
[4] J. F. Brown, Jr., *J. Am. Chem. Soc.* **1965**, *87*, 4317.
[5] F. J. Feher, D. A. Newman, J. F. Walzer, *J. Am. Chem. Soc.* **1989**, *111*, 1741.
[6] B. Hong, T. P. S. Thoms, H. J. Murfee, M. J. Lebrun, *Inorg. Chem.* **1997**, *36*, 6145.
[7] R. Bakhtiar, *Rapid Commun. Mass Spectrom.* **1999**, *13*, 87.
[8] R. Bakhtiar, F. J. Feher, *Rapid Commun. Mass Spectrom.* **1999**, *13*, 687.
[9] W. E. Wallace, C. M. Guttman, J. M. Antonucci, *J. Am. Soc. Mass Spectrom.* **1999**, *10*, 224.
[10] W. E. Wallace, C. M. Guttman, J. M. Antonucci, *Polymer* **2000**, *41*, 2219.
[11] P. Eisenberg, R. Erra-Balsells, Y. Ishikawa, J. C. Lucas, A. N. Mauri, H. Nonami, C. C. Riccardi, R. J. J. Williams, *Macromolecules* **2000**, *33*, 1940.
[12] L. Matejka, O. Dukh, J. Brus, W. J. Simonsick, Jr., B. Meissner, *J. Non-Cryst. Solids* **2000**, *270*, 34.
[13] K. Piana, U. Schubert, *Chem. Mater.* **1994**, *6*, 1504.
[14] A. N. Mauri, C. C. Riccardi, R. J. J. Williams, *Macromol. Symp.* **2000**, *151*, 331.
[15] R. Nass, E. Arpac, W. Glaubitt, H. Schmidt, *J. Non-Cryst. Solids* **1990**, *121*, 370.
[16] H. Nonami, S. Fukui, R. Erra-Balsells, *J. Mass Spectrom.* **1997**, *32*, 287.
[17] H. Nonami, K. Tanaka, Y. Fukuyama, R. Erra-Balsells, *Rapid Commun. Mass Spectrom.* **1998**, *12*, 285.
[18] A. N. Mauri, C. C. Riccardi, R. J. J. Williams, *Polym. Bull. (Berlin)* **2001**, *45*, 523.
[19] R. Erra-Balsells, A. Kolender, M. C. Matulewicz, H. Nonami, A. S. Cerezo, *Carbohydr. Res.* **2000**, *329*, 157.